A Novel Transmit Array Structure for Optical Spatial Modulation

A Novel Transmit Array Structure for Optical Spatial Modulation

Tezcan Cogalan*, Harald Haas* and Erdal Panayirci†

*School of Engineering
Institute for Digital Communications
Li-Fi R&D Centre, The University of Edinburgh
Edinburgh, EH9 3JL, UK
Email: {t.cogalan, h.haas}@ed.ac.uk

†Kadir Has University
Department of Electrical and Electronics Engineering
Istanbul, 34083, Turkey
Email: {eepanay}@khas.edu.tr

***Abstract*—The performance of multiple input single output (MISO) and multiple input multiple output (MIMO) systems is limited by spatial channel correlation. This limitation becomes more severe for light fidelity (LiFi) systems, which use intensity modulation/direct detection (IM/DD) for data transmission, due to lack of phase information and fading. This paper proposes a novel transmitter structure that provides spatially separated channels and enables optical MISO/MIMO spatial modulation (SM) transmission without the need for power allocation algorithm or a transmit precoding technique. A single light emitting diode (LED) array, which consists of multiple LEDs with different characteristics is considered in an indoor environment. Different numbers of transmit LEDs are chosen for SM transmission based on the relation between channel correlation and bit error probability. It is shown that the proposed structure provides reliable SM transmission when the number of transmit LEDs is considered as 2 and the modulation order for M-ary pulse amplitude modulation (PAM) is considered as 2 and 4. Computer simulations also show that higher modulation order, 8-PAM, can be supported with a cost of slightly higher bit error rate (BER) performance.**

I. Introduction

Light-fidelity (LiFi) is becoming a promising technology for indoor environments by using light-emitting diodes (LEDs) for illumination and data transmission simultaneously. Signal transmission in a LiFi system is performed by using intensity modulation (IM), which is a technique to convey information on the instantaneous optical power at the transmitter side, and by direct detection (DD) at the receiver side to convert the received optical intensity to an information signal dependent photo-current. As the data is modulated on to the instantaneous optical power, the transmit signal should be real-valued and non-negative. Therefore, well studied radio frequency (RF) based techniques need to be re-investigated for IM/DD LiFi systems.

In RF systems, employing multiple transmitters and receivers have been extensively studied to enhance the system capacity. It has been shown that increasing the number of transmit and/or receive elements improves the achievable data rates, substantially. Cross-talk between the transmit elements are mitigated by the processing, also known as precoding, that is employed at the transmitter side in both MISO and MIMO communications [1], [2]. In the precoding techniques, statistical properties of the RF channel due to fading is used to spatially separate the multiple channels. Additionally, the cross-talk problem in multiple input single output (MISO)/multiple input multiple output (MIMO) systems can also be mitigated by the spatial modulation (SM) technique. In SM, only a single transmit element is activated during a symbol transmission period where the index of the activated element, known as the spatial symbol, conveys extra information [2].

In IM/DD systems, channel gains rely on the geometry between the transmitter and receiver. Therefore, spatial channel correlation is the main limitation for MISO/MIMO IM/DD systems. Indoor MISO and/or MIMO IM/DD systems have been studied in [3]–[7] and in [8]–[12] in conjunction with SM. It is shown that the optical multi transmit element channel is highly correlated and, specifically, employing SM relies on appropriate design of transmitter and receiver [8], [10], [11]. The spatial correlation between optical channels is reduced either by power allocation algorithms which are proposed as part of the transmitter design [4]–[7], [11] or using some optical processing at the receiver side [3], [12].

In [6], [7], in addition to the power allocation algorithm, orientation of LEDs in an LED array is used to de-correlate the multi transmit element channel. It is shown in [3], [6], [7], [12] that changing the geometry of the transmitter and/or receiver side can provide nearly uncorrelated optical channels.

In this study, instead of designing a precoder and/or power control algorithm, a novel transmit LED array structure is proposed to provide a spatially uncorrelated optical multi transmit element channel. The optical SM studies presented in [8], [9], [12] consider multiple LED luminaries located as a grid in the ceiling of a room. Although a grid-based LED luminary placement is reasonable for office environments, most of the indoor environments are not suitable for employment of a grid-based luminary placement. Hence, in this study, a single LED luminary, consisting of multiple LEDs, is considered to employ SM and to provide the same illumination level throughout the indoor environment. For the

sake of comparison, the system model considered in [8] is adapted in this paper. Accordingly, performance of a unipolar M-ary pulse amplitude modulation (PAM) MIMO-SM system is investigated when the proposed transmitter structure is employed. The relationship between error probability and channel correlation of optical 2-PAM MISO-SM system given in [11] is extended for M-PAM when the channel gain of the transmit elements follows some specific properties.

This paper is organized as follows. The system model is described in detail in Section II. The relation between the channel gains and error performance is given in Section III. In Section IV, the proposed transmit LED array structure is described along with the channel model and how to select LEDs for transmission. The simulation parameters and results are presented in Section V. Finally, conclusions are presented in Section VI.

Notation: Throughout the paper, vectors and matrices are written in bold lower-case and upper-case letters, respectively. The transpose and Frobenius norm of a vector is expressed by $(.)^T$ and $\|.\|_{\mathrm{F}}$, respectively. Real normal distribution is given by $\mathcal{N}\left(\mu, \sigma^2\right)$ where μ represents mean and σ^2 is variance. $\mathbb{R}^+$ denotes the ring of positive real numbers. The argument of the minimum and maximum are represented by $\arg\min\{.\}$ and $\arg\max\{.\}$, respectively.

II. System Model

An optical MIMO system which uses IM and DD is considered in this paper. At the transmitter side, a LED array with multiple LEDs, consisting of N_l LEDs, is used for transmission of data with optical SM. N_t of N_l LEDs are chosen for SM, and unipolar M-PAM is employed. It is assumed that the LED array is located in the middle of a room. At the receiver side, a single user, with N_p multiple photo diodes (PDs), is assumed at different locations inside the room. Accordingly, the received signal $\boldsymbol{y}$ can be written as in a vector form as follows:

$$\boldsymbol{y} = \hat{\boldsymbol{H}}\boldsymbol{s} + \boldsymbol{n}, \tag{1}$$

where $\hat{\boldsymbol{H}} \in \mathbb{R}^{+}_{N_p \times N_t}$ is the optical channel gain matrix, which is a sub-matrix of $\boldsymbol{H} \in \mathbb{R}^{+}_{N_p \times N_l}$; $\boldsymbol{s} \in \mathbb{R}^{+}_{N_t \times 1}$ is the transmitted signal vector; and $\boldsymbol{n} \in \mathbb{R}_{N_p \times 1}$ is the additive white Gaussian noise (AWGN) vector where each element of $\boldsymbol{n}$ is independently distributed with $\mathcal{N}\left(0, \sigma^2\right)$. In this paper, without loss of generality, the optical-to-electrical (O/E) and electrical-to-optical (E/O) conversion coefficients are assumed to be unity.

When SM is employed in a system, transmit data is encoded both as spatial and PAM constellation symbols. Since, only one of the LEDs is activated during transmission, the overall spectral efficiency of the system is $\log_2(N_t) + \log_2(M)$ bits/s/Hz.

As noted in [8], a signal constellation with zero intensity cannot be used in optical SM, due to the fact that there would not be an active transmit element and hence no spatial information exist. In this paper, the intensity levels of M-PAM signals for optical SM are given as:

$$I_m^M = \frac{I}{M}(2m-1) \quad \text{for} \quad m = 1, 2, \ldots, M, \tag{2}$$

where I is the average emitted optical power. The present equation (2) is different from the one used in [8]. In [8], the distance between the intensity levels is smaller than the given intensity levels in (2). Therefore, it can be expected that the bit error probability of the system is higher in [8] for the same intensity range. Accordingly, the transmit LED is activated based on the spatial symbol and the intensity level of the transmit LED is decided according to the constellation symbol. Interested readers can be referred to [8, Fig. 2] to understand the described M-PAM-optical SM model. For example, if a symbol representing the bit sequence "100" is going to be transmitted over an optical SM system with $N_t = 2$ and $M = 4$, the spatial symbol "1" activates LED_2 and the intensity level I_1^4 is chosen to transmit the constellation symbol "00". Accordingly, the transmit vector can be written as $\boldsymbol{s} = \left[0, I_1^4\right]^{\mathrm{T}}$.

III. Minimum Error Performance

As the spatial symbol decides which LED is activated to transmit the M-PAM symbol, the error probability depends highly on estimating the correct index of the activated LED. Hence, correlation among N_t transmit LEDs effects directly on the error performance of an optical SM system. Once the correct LED index is estimated, the error performance becomes dependent on the received signal-to-noise ratio (SNR) to decode the M-PAM symbols correctly. In SM systems, the spatial and M-PAM constellation symbols are jointly estimated by the maximum likelihood (ML) detector at the receiver follows [8]:

$$\hat{s} = \arg\max_{\boldsymbol{s}} p_{\boldsymbol{y}}\left(\boldsymbol{y}|\boldsymbol{s}, \hat{\boldsymbol{H}}\right) = \arg\min_{\boldsymbol{s}} \left\|\boldsymbol{y} - \hat{\boldsymbol{H}}\boldsymbol{s}\right\|_{\mathrm{F}}^2, \tag{3}$$

where $p_{\boldsymbol{y}}$ is the probability density function of the received vector $\boldsymbol{y}$, conditioned on the transmit vector $\boldsymbol{s}$ and the optical channel gain matrix $\hat{\boldsymbol{H}}$. Accordingly, the Euclidean distance between the received vector and all possible symbol transmissions is minimized by the ML detector. It is assumed that the transmitter and receiver have perfect channel state information (CSI). At the transmitter, CSI is used to choose optimal N_t out of N_l LEDs to achieve the best minimum distance at the receiver side. For the sake of simplicity, it is assumed that the optical channel gains between transmitter and the N_p PDs are the same. Hence, during the bit error rate (BER) calculations, the $N_t \times N_p$ MIMO system is considered as if it is an $N_t \times 1$ MISO system. Based on the Frobenius norm in (3), the ML detector then evaluates the summation of the square of N_p observations and yields an optimal decision regarding the detected symbol transmitted.

As it is shown in [11], the simplified symbol error rate (SER) for the $N_t \times 1$ M-PAM optical SM system can be

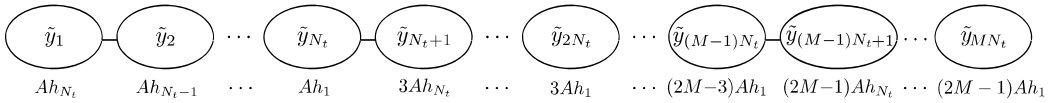

Fig. 1. Received symbols constellation in the presence of noise. A represents I/M in (2).

computed as:

$$\mathrm{SER} = \frac{2}{K}\sum_{r=1}^{K-1} Q\left(\frac{d_{r,r+1}}{2\sigma}\right), \tag{4}$$

where $d_{r,r+1}$ is the Euclidean distance between the r^{th} and $(r+1)^{\text{th}}$ adjacent constellation points. $r = 1, 2, \ldots, K$ is the symbol index and K represents the combination of the spatial and constellation symbols with $K = MN_l$; and $Q(x) = \frac{1}{\sqrt{2\pi}}\int_x^\infty \exp^{-(u^2/2)}\,\mathrm{d}u$.

In this paper, it is assumed that $h_1 > h_2 > \ldots > h_{N_t}$ and $I_{m'}^{M} h_1 < I_{m'+1}^{M} h_{N_t}$ where $m' = 1, 2, \ldots, M-1$. According to the given assumption and when the noise is not present, the received signals, $\tilde{\boldsymbol{y}}$, are shown in Fig. 1, in ascending order. The Euclidean distance between the symbols can be obtained by $d_{r,r+1} = \tilde{y}_{r+1} - \tilde{y}_r$. Consequently, the received symbol constellation diagram, given, can only be evaluated when the correlation between the maximum and minimum channel gains of the selected N_t LEDs is:

$$\frac{(2M-3)}{(2M-1)} h_1 \leq h_{N_t}. \tag{5}$$

IV. Transmitter Structure

Existing light fixtures consist of a different number of LEDs depending on the manufacturer's design. In this study, a LED array consisting of N_l LEDs is considered for the purpose of showing the proof of concept when the number of selected LEDs for transmission is assumed to be 2 ($N_t = 2$). As it is noted, the performance of a SM system is highly dependent on the correlation among the transmit elements. Therefore, the transmitter array proposed in this study aims to decrease the correlation among LEDs by manipulating the array geometry. It is important to note that the main functionality of the LED luminaries is to provide uniform illumination in the environment. Data transmission through LEDs is an additional functionality. Thus, the proposed transmitter structure should firstly provide the desired illumination level. Then, the performance of the data transmission should be taken into account.

In order to provide a uniform illumination level through the 4 m $\times$ 4 m $\times$ 3 m room, the LEDs in the array should be oriented in different directions and should have the same channel gain through their orientation. Possible orientation of the LEDs that illuminate the environment is illustrated in Fig. 2. The optical channel gain at point X_i from LED_i is expressed by Lambertian reflection as:

$$G_{X_i,i} = \frac{(m_i+1)\,A_{R_x} G_{R_x}}{2\pi\left(|OX_i|\right)^2}\cos^{m_i}\left(\phi_{X_i,i}\right)\cos\left(\psi_{X_i,i}\right) R, \tag{6a}$$

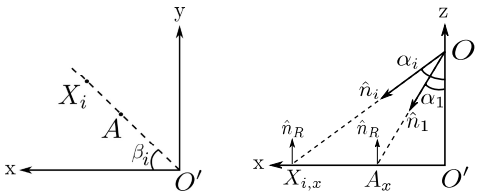

(a) XY-axes (b) XZ-axes

Fig. 2. Illustration of orientation of LEDs. β_i and $\hat{n}_i$ represent horizontal orientation and normal of LED_i, respectively; $\hat{n}_R$ represents normal of the receiver; and A_x represents x-axis component of the point A.

$$R = \mathrm{rect}\left(\frac{\psi_{X_i,i}}{\mathrm{FOV}_{R_x}}\right), \tag{6b}$$

$$m_i = -\ln 2 / \ln\left(\cos\left(\Psi_{\frac{1}{2},i}\right)\right), \tag{6c}$$

where i represents LED index ($i = 1, \ldots, N_l$); m_i is the Lambertian order and depends on the semi-angle of the LED_i, $\Psi_{\frac{1}{2},i}$, as given in (6c); $|OX_i|$ represents the distance between points O and X_i; $\phi_{X_i,i}$ is the divergence angle from LED_i to receiver at the point X_i based on the normal of the LED_i; $\psi_{X_i,i}$ is the incidence angle from LED_i to receiver at the point X_i based on the normal of the receiver; G_{R_x} is the optical filter gain; A_{R_x} is the area of the receiver; and R is 0 or 1 according to ratio of the incidence angle and field-of-view (FOV) of the receiver, FOV_{R_x}. If the absolute value of the ratio is smaller than or equal to 1, the rect function gives 1 and otherwise, it gives 0. As explained in [8], reflected optical paths can be neglected. Thus, only line of sight (LoS) links are considered in this paper.

When the room height ($|OO'|$), semi-angle ($\Psi_{\frac{1}{2},1}$) and horizontal orientation (β_1) of LED_1 are assumed to be known and $\mathrm{FOV}_{R_x} = 90°$, the vertical orientation of LED_1 can be computed as follows:

- *Consider $G_{O',1} = \frac{1}{k} G_{A,1}$ to find α_1 which is considered as larger than $0°$ in order to break the symmetry in the room,*

$$G_{O',1} = \frac{(m_1+1)}{2\pi(|OO'|)^2}\cos^{m_1}(\phi_{O',1})\cos(\psi_{O',1}), \tag{7}$$

$$\frac{1}{k} G_{A,1} = \frac{1}{k}\frac{(m_1+1)}{2\pi(|OA|)^2}\cos^{m_1}(\phi_{A,1})\cos(\psi_{A,1}), \tag{8}$$

where $\phi_{A,1} = \psi_{O',1} = 0°$; $\phi_{O',1} = \psi_{A,1} = \alpha_1$ and $\cos(\alpha_1) = |OO'|/|OA|$. Thus, (7) can be written as:

$$\frac{\cos(\alpha_1)}{k\frac{|OO'|^2}{\cos^2(\alpha_1)}} = \frac{\cos^{m_1}(\alpha_1)}{|OO'|^2}, \tag{9a}$$

$$\frac{1}{k} = \cos^{m_1-3}(\alpha_1), \tag{9b}$$

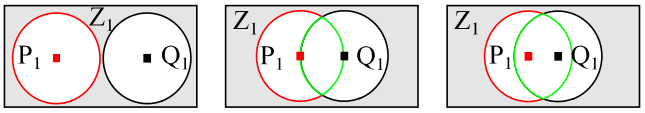

(a) Case 1 (b) Case 2 (c) Case 3

Fig. 3. Normalized channel gain distribution of LED_2 and LED_4 in case of $N_t = 2$ and $N_t = 4$ transmission when the LED array is designed for 2-PAM and 8-PAM, respectively.

$$\cos(\alpha_1) = \left(\frac{1}{k}\right)^{\left(\frac{1}{m_1-3}\right)}, \tag{9c}$$

$$\alpha_1 = \arccos\left(\frac{1}{k}\right)^{\left(\frac{1}{m_1-3}\right)}. \tag{9d}$$

According to (5), the channel gain of LED_{N_t} should be larger than $1/k \in \{1/3, 5/7, 13/15\}$ of the channel gain of LED_1 to support 2-PAM, 4-PAM or 8-PAM, respectively. In Fig. 3, three different cases are considered to decide how to chose center location of LEDs in a horizontal orientation β_i. In all three cases, the sets P_1, Q_1 and Z_1 represent $h_j > 1/k$, $h_{j-1} > 1/k$ and $h_j, h_{j-1} < 1/k$, respectively. The intersection of sets P_1 and Q_1 is $P_1 \cap Q_1 = \emptyset$ for the case 1 and $P_1 \cap Q_1 > 0$ for the cases 2 and 3. Inherently, $P_1 \cap Q_1$ in the case 3 is larger than the case 2. However, considering the case 3 may result excessive number of LEDs to be deployed for a single horizontal orientation. In this paper, the case 2 is used to decide the center of LEDs in a horizontal orientation. In order to deploy LEDs based on the case 2, the location where the maximum channel gain is decreased by $1/k$ is chosen as the center of another cell, as depicted in Fig. 3. Accordingly, once the orientation of LED_1 is found, the characteristics of the remaining LEDs can be found based on the ratio $1/k$. The Lambertian order and orientation of the remaining LEDs can be obtained as follows:

- *Consider* $(1/k)\, G_{A,1} = G_{B,1}$ *where* B *is the center location of* LED_2, $X_{i=2}$ *to find* α_2, $(\alpha_2 > \alpha_1)$

$$(1/k)\, G_{A,1} = \frac{1}{k}\frac{(m_1+1)}{2\pi(|OA|)^2}\cos^{m_1}(\phi_{A,1})\cos(\psi_{A,1}), \tag{10a}$$

$$G_{B,1} = \frac{(m_1+1)}{2\pi(|OB|)^2}\cos^{m_1}(\phi_{B,1})\cos(\psi_{B,1}), \tag{10b}$$

where $\phi_{A,1} = 0°$; $\psi_{A,1} = \alpha_1$; $\phi_{B,1} = \alpha_2 - \alpha_1$; $\psi_{B,1} = \alpha_2$; and $\cos(\alpha_2) = |OO'|/|OB|$. Hence, (10) can be written as:

$$\frac{1}{k}\cos^3(\alpha_1) = \cos^{m_1}(\alpha_2 - \alpha_1)\cos^3(\alpha_2), \tag{11a}$$

$$\left(\frac{1}{k}\frac{\cos^3(\alpha_1)}{\cos^3(\alpha_2)}\right)^{\left(\frac{1}{m_1}\right)} = \cos(\alpha_2 - \alpha_1), \tag{11b}$$

$$\arccos\left(\left(\frac{1}{k}\frac{\cos^3(\alpha_1)}{\cos^3(\alpha_2)}\right)^{\left(\frac{1}{m_1}\right)}\right) = (\alpha_2 - \alpha_1), \tag{11c}$$

where the difference between orientation angle of LEDs can be generalized by replacing subscripts 1 and 2 with $j-1$ and j, respectively, in (11c) as:

$$\arccos\left(\left(\frac{1}{k}\frac{\cos^3(\alpha_{j-1})}{\cos^3(\alpha_j)}\right)^{\left(\frac{1}{m_{j-1}}\right)}\right) = (\alpha_j - \alpha_{j-1}). \tag{12}$$

- *Consider* $G_{A,1} = G_{X_j,j}$ *to find* m_j. *It can be said that the divergence and incidence angles are* $\phi_{A,1} = \phi_{X_j,j} = 0°$ *and* $\psi_{X_j,j} = \alpha_j$, *respectively; and* $\cos(\alpha_j) = |OO'|/|OX_j|$. *The Lambertian order of* LED_j *can be calculated by using* (6a) *as:*

$$\frac{(m_1+1)\cos(\alpha_1)}{|OA|^2} = \frac{(m_j+1)\cos(\alpha_j)}{|OX_j|^2}, \tag{13a}$$

$$\frac{(m_1+1)\cos^3(\alpha_1)}{|OO'|^2} = \frac{(m_j+1)\cos^3(\alpha_j)}{|OO'|^2}, \tag{13b}$$

$$m_j = \frac{(m_1+1)\cos^3(\alpha_1)}{\cos^3(\alpha_j)} - 1 \tag{13c}$$

In this work, the Lambertian order of the LEDs are constrained to having an integer-valued semi-angle. Based on (11c), α_2 is a function of α_1 where α_1 is a function of m_1. An integer-valued semi-angle for $\text{LED}_{j=2}$ is found by:

$$\underset{\alpha_j, m_j}{\text{minimize}} \quad \left(\Psi_{\frac{1}{2},j} - \text{round}\left(\Psi_{\frac{1}{2},j}\right)\right)^2 \tag{14a}$$

$$\text{subject to} \quad (9\text{d}), (12), (13\text{c}), \quad \forall j, \tag{14b}$$

$$45° > \alpha_j > \alpha_{j-1} > 0°, \quad \forall j > 1, \tag{14c}$$

$$\alpha_j - \alpha_{j-1} > \Psi_{\frac{1}{2},j-1}, \quad \forall j > 1, \tag{14d}$$

where the function round (.) rounds a value to its lower or higher integer number. The constraint given in (14c) ensures that the LED_j is not oriented to one of the side walls of the environment. Similarly, the constraint given in (14d) ensures that the orientation of the next LED is in the coverage area of the previous LED in order to have overlapped cells, as shown in Fig. 3(b). The orientation and Lambertian order, inherently the semi-angle, of $\text{LED}_{j>1}$ at one horizontal resolution can be obtained by (14). Once the characteristics of the LEDs at $\beta = 0°$ are found, the characteristics of the remaining LEDs can be obtained by shifting the horizontal orientation by β_b, as described in Algorithm 1.

The vertical orientation, semi-angle and center location of the LEDs for the horizontal orientation $\beta = 0°$ are given when the modulation order is considered as $M = 2$ in Table I and as $M = 8$ in Table II.

A. Selection of Transmit LEDs

The transmit LED selection process used in this study is based on (5). Firstly, the LED, which provides the highest channel gain for a given receiver location, is chosen as LED_1. Then, based on the considered number of transmit LEDs N_t

Algorithm 1 LED Array Design

Require: Modulation order (M); semi-angle of LED$_1$ $\left(\Psi_{\frac{1}{2},1}\right)$; and angular resolution of horizontal orientation (β_b);

Ensure: Orientation of an LED is not larger than $45°$; semi-angle of LED$_j$ $\left(\Psi_{\frac{1}{2},j}\right)$ is integer valued; and $(\alpha_j - \alpha_{j-1}) \leq \Psi_{\frac{1}{2},j-1}$;

Initialization;

Determine the maximum channel gain decrease ratio by (5);

Find α_1 by (9d);

$\beta_1 \leftarrow 0°$;

$j \leftarrow 2$;

while $\alpha_{j-1} < 45°$ **do**

  Find α_j, m_j and $\Psi_{\frac{1}{2},j}$ by (14);

  $\beta_j = \beta_{j-1}$;

  $j \leftarrow j + 1$;

end while

Determine number of LEDs per horizontal resolution $N_{l,\beta} \leftarrow j - 1$;

$i \leftarrow j$

$\beta_i \leftarrow \beta_j + \beta_b$

while $\beta_i \leq (360° - \beta_b)$ **do**

  for $k = 1, \ldots N_{l,\beta}$ **do**

    $\alpha_i = \alpha_k$; $\beta_i = \beta_k$; $m_i = m_k$; $\Psi_{\frac{1}{2},i} = \Psi_{\frac{1}{2},k}$;

    $i \leftarrow i + 1$;

  end for

  $\beta_i \leftarrow \beta_i + \beta_b$;

end while

Obtain number of LEDs, $N_l \leftarrow i$.

TABLE I
LED CHARACTERISTICS FOR 2-PAM, $\beta = 0°$

LED$_j$	1	2	3
α_j	17.3°	31°	42.9°
$\Psi_{\frac{1}{2},j}$	13°	11°	9°

and constellation size M, N_t LEDs are chosen in a way that satisfies $h_1 > h_2 > \ldots > h_{N_t}$ and (5).

V. System Simulation Results

In the computer simulations, the system model given in [8] is used with some modifications. Accordingly, the receiver is assumed to have $N_p = 4$ PDs which are located on the corners of a square with side length of 0.1 m. All the PDs are pointed upwards, assumed to have 45° FOV ($\text{FOV}_{R_x} = 45°$) and the receiver height is considered as 0.75 m. Without loss of generality, the optical filter gain G_{R_x} and the area of the receiver A_{R_x} are taken as 1 and 1 cm^2, respectively to simplify the analysis. The transmitter is assumed to have a structure as described in Table I for $M = 2$ and in Table II for $M = 8$. The horizontal resolution β_b is chosen as 15°. The LED array consists of $N_l = 72$ and $N_l = 192$ LEDs for $M = 2$ and $M = 8$, respectively. The room is divided into 27×27 pixels[1] where the receiver is located at the center of each pixel. To obtain average BER performance, randomly generated spatial and constellation symbol sets are iterated 10^5 times for each receiver location.

TABLE II
LED CHARACTERISTICS FOR 8-PAM, $\beta = 0°$

LED$_j$	1	2	3	4	5	6	7	8
α_j	11.5°	17.7°	22.8°	27.2°	31°	34.4°	37.5°	40.3°
$\Psi_{\frac{1}{2},j}$	21°	20°	19°	18°	17°	16°	15°	14°

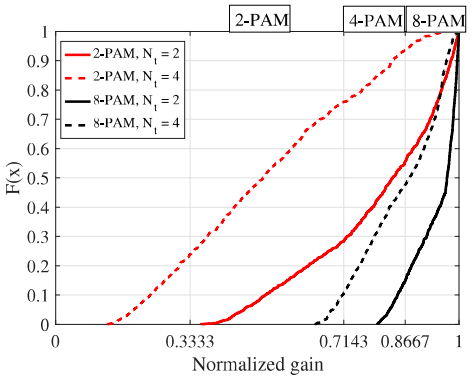

Fig. 4. Normalized channel gain distribution of LED$_2$ and LED$_4$ in case of $N_t = 2$ and $N_t = 4$ transmission when the LED array is designed for 2-PAM and 8-PAM, respectively.

The SNR is defined based on the received signal power and assumed having the same SNR level irrespective of the receiver location. Therefore, the noise power is generated based on the given SNR as $\sigma^2 = 1/\text{SNR}$. Additionally, as noted earlier, only the LoS link is considered in the channel gain calculation.

In Fig. 4, cumulative distribution function (CDF) of the normalized channel gain of the LED$_{N_t}$ is shown for $N_t = 2$ and $N_t = 4$ when LED array is designed for $M = 2$ and $M = 8$. The normalized channel gain is obtained by dividing the achieved channel gain of the LEDs with the gain of LED$_1$, which is the maximum achieved gain for a given receiver location. Hence, based on (5), the channel gain of LED$_{N_t}$ should be larger than $1/3$, $5/7$ and $13/15$ of the channel gain of the LED$_1$ for 2-PAM, 4-PAM and 8-PAM, respectively. Also, the channel gain of LED$_{N_t}$ should be smaller than 1 to satisfy $h_1 > h_{N_t}$. According to Fig. 4, when the LED array is designed for $M = 2$, the inequality given by (5) is satisfied for around 99%, 69% and 40% of the illuminated area when the system with $N_t = 2$ is considered with 2-PAM, 4-PAM and 8-PAM optical SM transmission, respectively. However, when the system with $N_t = 4$ is considered, 2-PAM transmission can be supported by 75% of the illuminated area for the given transmitter structure. When the design is carried out for $M = 8$, it is shown that 8-PAM optical SM transmission can be used around 85% and 50% of the illuminated area for $N_t = 2$ and $N_t = 4$, respectively.

[1]This is equivalent to sliding the square receiver through the room.

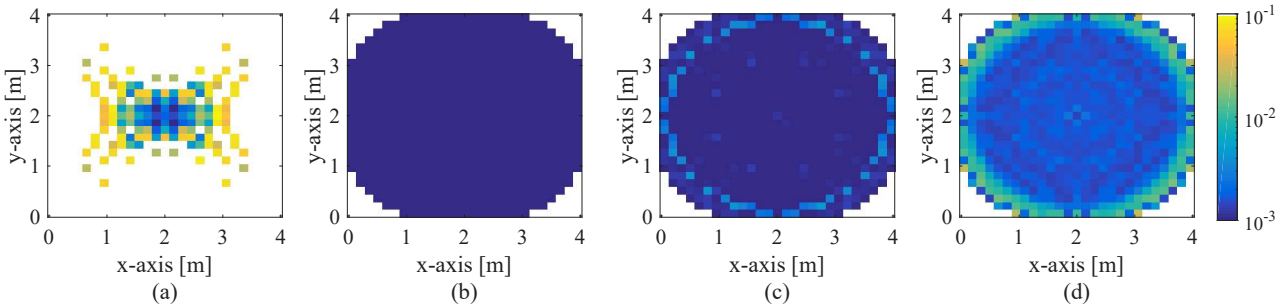

Fig. 5. Average BER performance inside the room when the received SNR is considered as 30 dB. White areas represent either BER higher than 0.18 or no channel gain. (a) $N_t = 4$, 2-PAM [8]. (b) $N_t = 2$, 2-PAM. (c) $N_t = 2$, 4-PAM. (d) $N_t = 2$, 8-PAM.

In Fig. 5, the average BER performance of different optical SM systems are investigated when the received SNR is considered as 30 dB. In Fig. 5(a), the performance of the system proposed in [8] is shown. This is a 4×4 MIMO-optical SM system with 2-PAM where $N_t = 4$ LEDs are located 0.6 m apart from each other as explained in detail in [8]. The spectral efficiency of the system in [8] is 3 bits/s/Hz. It is important to note that in [8], $\mathrm{FOV}_{\mathrm{R_x}}$ is considered as 15° for all PDs and 4-PAM is used as the modulation order. In order to investigate the BER performance all over the room, a larger $\mathrm{FOV}_{\mathrm{R_x}}$ is needed. Therefore, the system model given in [8] is used with $\mathrm{FOV}_{\mathrm{R_x}}$ modification in this study. As it can be seen from the figure, the system achieves low BER performance only at the center of the room. In the rest of the room, the BER is above 10^{-1}. When the proposed transmit structure is considered in a 2×4 MIMO-optical SM system with 4-PAM, the same spectral efficiency is achieved notably in a larger area than the system given in [8] as shown in Fig. 5(c). In Fig. 5(b), it can be seen that the spectral efficiency of 2 bits/s/Hz can be achieved error-free in the most of the room. Also, it is shown in Fig. 5(d) that the BER performance of the system with 8-PAM is slightly above 10^{-3}.

VI. Conclusions

In this paper, a novel LED array structure is proposed to enable reliable optical MIMO-SM transmission without needing a power allocation algorithm or precoding technique. A single LED array, which consists of multiple LEDs with different characteristics, is used for both illumination and simultaneous data transmission. A relationship between error probability and channel correlation is provided for M-ary PAM-SM system. Based on the given relation, the LED array is designed to separate multiple channels. It has been demonstrated that channel correlation can be reduced by manipulating the transmitter geometry and SM can be employed for IM/DD based systems. Simulation results show that the proposed structure can achieve decent BER performance for a single user inside a 4 m $\times$ 4 m $\times$ 3 m room. For future studies, the proposed structure can be investigated for a case of multiple users, where spatially separated users can be served reliably.

Acknowledgement

Prof. Haas acknowledges support from the Engineering and Physical Sciences Research Council (EPSRC) under the Established Career Fellowship grant EP/R007101/1. He also acknowledges the financial support of his research by the Wolfson Foundation and the Royal Society. Prof. Panayirci acknowledges support from the Scientific and Technological Research Council of Turkey (TUBITAK) under the 1003-Priority Areas R&D Projects Support Program No. 118E559.

References

[1] M. Joham, W. Utschick, and J. Nossek, "Linear Transmit Processing in MIMO Communications Systems," *IEEE Trans. Signal Processing*, vol. 53, no. 8, pp. 2700–2712, Aug 2005.

[2] M. Di Renzo, H. Haas, A. Ghrayeb, S. Sugiura, and L. Hanzo, "Spatial Modulation for Generalized MIMO: Challenges, Opportunities, and Implementation," *Proc. IEEE*, vol. 102, no. 1, pp. 56–103, Jan. 2014.

[3] A. Nuwanpriya, S. W. Ho, and C. S. Chen, "Indoor MIMO Visible Light Communications: Novel Angle Diversity Receivers for Mobile Users," *IEEE J. Sel. Areas Commun.*, vol. 33, no. 9, pp. 1780–1792, Sept. 2015.

[4] K.-H. Park, Y.-C. Ko, and M. Alouini, "On the Power and Offset Allocation for Rate Adaptation of Spatial Multiplexing in Optical Wireless MIMO Channels," *IEEE Trans. Commun.*, vol. 61, no. 4, pp. 1535–1543, April 2013.

[5] H. Ma, L. Lampe, and S. Hranilovic, "Robust MMSE Linear Precoding for Visible Light Communication Broadcasting Systems," *IEEE Globecom Workshops*, pp. 1081–1086, Dec 2013.

[6] T. Cogalan, H. Haas, and E. Panayirci, "Power Control-Based Multi-User Li-Fi Using a Compound Eye Transmitter," in *2015 IEEE Global Communications Conference (GLOBECOM)*, Dec 2015, pp. 1–6.

[7] J. Lian and M. Brandt-Pearce, "Distributed Power Allocation for Multiuser MISO Indoor Visible Light Communications," in *2015 IEEE Global Communications Conference (GLOBECOM)*, Dec 2015, pp. 1–7.

[8] T. Fath and H. Haas, "Performance Comparison of MIMO Techniques for Optical Wireless Communications in Indoor Environments," *IEEE Trans. Commun.*, vol. 61, no. 2, pp. 733–742, February 2013.

[9] R. Mesleh, H. Elgala, and H. Haas, "Optical Spatial Modulation," *IEEE/OSA J. Opt. Commun. Networking*, vol. 3, no. 3, pp. 234–244, March 2011.

[10] W. O. Popoola, "Merits and Limitations of Spatial Modulation for Optical Wireless Communications," in *2013 2nd International Workshop on Optical Wireless Communications (IWOW)*, Oct 2013, pp. 152–156.

[11] A. Yesilkaya, T. Cogalan, E. Panayirci, H. Haas, and H. V. Poor, "Achieving Minimum Error in MISO Optical Spatial Modulation," in *2018 IEEE International Conference on Communications (ICC)*, May 2018, pp. 1–6.

[12] J. Lian and M. Brandt-Pearce, "Multiuser MIMO Indoor Visible Light Communication System Using Spatial Multiplexing," *J. Lightwave Technol.*, vol. 35, no. 23, pp. 5024–5033, Dec 2017.